

# Study of tip loss corrections using CFD rotor computations

W Z Shen<sup>1</sup>, W J Zhu<sup>1</sup>, and J N Sørensen<sup>1</sup>

<sup>1</sup>Department of Wind Energy, Technical University of Denmark, DK-2800 Lyngby, Denmark

E-mail: wzsh@dtu.dk

**Abstract.** Tip loss correction is known to play an important role for engineering prediction of wind turbine performance. There are two different types of tip loss corrections: tip corrections on momentum theory and tip corrections on airfoil data. In this paper, we study the latter using detailed CFD computations for wind turbines with sharp tip. Using the technique of determination of angle of attack and the CFD results for a NordTank 500 kW rotor, airfoil data are extracted and a new tip loss function on airfoil data is derived. To validate, BEM computations with the new tip loss function are carried out and compared with CFD results for the NordTank 500 kW turbine and the NREL 5 MW turbine. Comparisons show that BEM with the new tip loss function can predict correctly the loading near the blade tip.

## 1. Introduction

A wind turbine usually is equipped with two or three blades and each turbine blade contains a tip where the flow from the pressure and suction sides meets together so that the pressure equalizes at the tip. This pressure equalization at the tip produces the effects that the loading at the tip cross-section equals to zero, the flow at the cross-sections near the blade tip is different than the two-dimensional flows and the loading at these cross-sections is smaller than that in the two-dimensional flows.

Previous studies on tip loss correction were carried out by Shen *et al.* [1, 2] where the NREL experimental rotor [3] and the Swedish WG 500 rotor [4] were considered. A correction function between the loading on a rotating blade and on a two-dimensional airfoil was derived. As these two rotors have blunt tip, the derived function can be used for rotors with blunt tip. In order to further extend the function, here we consider wind turbine rotors with sharp tip. As there are no detailed measurements available, we employ CFD computations to investigate the tip loss effects. The advantage of using CFD computations is that it can give very detailed information of the flow in the blade tip region. The NordTank 500 kW turbine and the virtual NREL 5 MW wind turbine have been studied here.

The procedure of the study is divided into five steps. First, CFD computations of the two rotors are carried out. Second, post-processing on determining the angle of attack for the NordTank 500 kW turbine is performed using the technique developed in [5]. Third, the tip loss function on airfoil data F1 is derived and verified with the derived lift-drag characteristics at the blade tip. Fourth, the tip loss function is implemented into a Blade Element Momentum (BEM) code. Finally, validations of the



BEM results are carried out against CFD results for the NordTank 500 kW and the virtual NREL 5 MW turbine.

## **2. Short description of the CFD computations**

To conduct CFD computations, we employ EllipSys3D code [6, 7]. The EllipSys3D code is based on a multi block / cell-centered finite volume discretization of the steady / unsteady incompressible Navier-Stokes equations in primitive variables (pressure-velocity). The predictor-corrector method is used. In the predictor step, the momentum equations are discretized by using a second-order backward differentiation scheme in time and second-order central differences in space, except for the convective terms that are discretized by the QUICK upwind scheme. In the corrector step, the improved Rhie-Chow interpolation developed by Shen *et al.* [8] is used in order to avoid numerical oscillations from velocity-pressure decoupling. The obtained Poisson pressure equation is solved by a five-level multi-grid technique. For more details about the numerical technique, the reader is referred to the references [6-8]. Since the EllipSys3D code is programmed with multi-block topology, it can be parallelized relatively easily using Message Passing Interface (MPI). As the flow past a wind turbine is often turbulent, a turbulence model needs to be combined with the Navier-Stokes code. In this study, we use the  $k-\omega$  SST turbulence model of Menter [9] and perform fully turbulent computations.

## **3. Short description of the technique of determination of angle of attack**

For a 2D airfoil the angle of attack (AOA) is defined as the geometrical angle between the flow direction and the chord. The concept of angle of attack is widely used in aero-elastic engineering models as an input to tabulated airfoil data that normally are established through a combination of wind tunnel tests and corrections for the effect of Coriolis and centrifugal forces in a rotating boundary layer. For a rotating blade the flow passing by a blade section is bended due to the rotation of the rotor, and the local flow field is influenced by the bound circulation on the blade. As a further complication, 3D effects from tip and root vortices render a precise definition of the AOA difficult. In [5] two simple methods are proposed to compute correctly the angle of attack for wind turbines in standard operations and in general flow conditions. For more details, the reader is referred to [5].

## **4. Short description of BEM with tip loss correction**

To take into account the difference between the physics of an actuator disc “with infinitely many blades” and an actual wind turbine or propeller with a finite number of blades, Prandtl [10] introduced the concept of tip loss and showed that the circulation of a real rotor tends to zero exponentially when approaching the blade tip. Glauert [11] used the Blade Element Momentum (BEM) theory as a computational tool to predict aerodynamic loading and power (see also Hansen [12]). The theory is based on one-dimensional momentum theory in which forces are distributed continuously in the azimuth direction. In order to render BEM computations more realistic, Glauert corrected the induced velocity in the momentum equations by exploiting the fact that the ratio between the averaged induced velocity and the induced velocity at the blade position tends to zero at the tip by the expression developed by Prandtl. A refined tip loss model was later introduced by Wilson-Lissaman [13] who suggested that the mass flow through the rotor disc should be corrected in the same manner as the induced velocity in the wake. This, however, leads to a formulation in which the orthogonality of the induced velocity to the relative velocity at the blade element is not satisfied. In order to satisfy the orthogonality condition, De Vries [14] refined further the tip correction of Wilson-Lissaman by correcting the mass flux in the tangential momentum equation in the same way as in the axial momentum equation.

Theoretical analyses and comparisons with measurements were carried out in [1] and showed that the existing tip loss corrections are inconsistent and fail to predict correctly the physical behaviour in the proximity of the tip. In order to overcome the difficulty, a new tip correction was proposed in [1]

where 2D force coefficients should include further the tip loss effects at the blade tip (corrected 2D force coefficients). This relation between uncorrected and corrected force coefficients was proposed as

$$C_n^r = F_1 C_n, \quad (1)$$

$$C_t^r = F_1 C_t, \quad (2)$$

The function F1 is

$$F_1 = \frac{2}{\pi} \cos^{-1} \left[ \exp\left(-g \frac{B(R-r)}{2R \sin \phi_R}\right) \right], \quad (3)$$

$$g = \exp(-0.125(B\lambda - 21)) + 0.1. \quad (4)$$

where  $B$  is the number of blades,  $R$  is the rotor radius,  $\phi_R$  is the flow angle at tip, and  $\lambda$  is tip-speed-ratio. The coefficients in F1 function were adjusted using the experimental data for flows past the NREL experimental rotor and the Swedish WG 500 rotor.

## 5. Results

In this section, we present first the CFD results of flows past the Nordtank 500 kW turbine. Next, we present the improved new tip loss function. Then, BEM results with the new tip loss function are compared with the CFD results of flows through the Nordtank 500 kW turbine and through the virtual NREL 5 MW turbine.

### 5.1. Results from CFD computations of the Nordtank 500 kW turbine

In this section, flows past the NordTank 500 kW turbine are computed using fully turbulent steady RANS computations. Although RANS has some difficulties to predict aerodynamic behaviours at high angles of attack, RANS is still a common tool for predicting the performance of wind turbines. The mesh used for the NordTank 500 kW rotor contains only one LM19.1 blade where periodic boundary conditions are used to represent the influence from the other two blades. The mesh is spherical and generated from a blade surface mesh of 5 blocks of 64x64 in a spherical domain with radius of 215 m which is about 5 rotor diameters. To ensure a good resolution near the blade, the height of the first cells near wall is kept to be below  $10^{-5}$  m. The total number of mesh points is about  $2.1 \times 10^6$ . As the flows become unsteady for wind speeds above 12 m/s, we restrict our computations for the rotor at wind speeds of 5, 6, 7, 8, 10, 12 m/s. The NordTank 500 kW turbine has a diameter of 41 m and rotates with a rotational speed of 27.1 RPM. In Figure 1, the limiting streamlines are shown for wind speeds of 7, 10 and 12 m/s. From the figure, it can be seen that the flow at 7 m/s is attached on the most part of the blade with a small separated region near the root. The flow separation region increases when the wind speed increases. At a wind speed of 12 m/s, more than half of the blade is stalled.

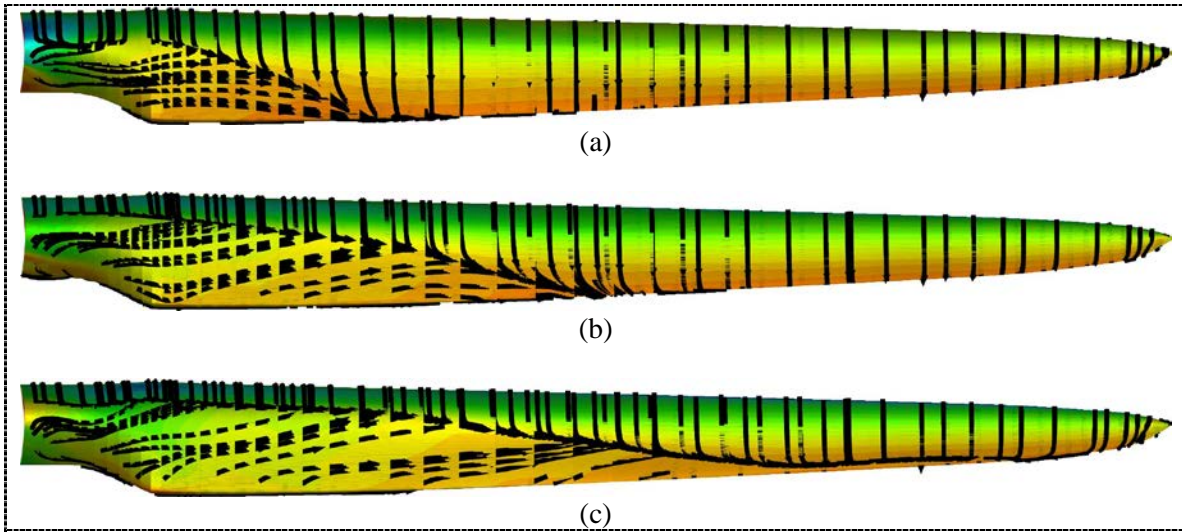


**Figure 1.** Limiting streamlines on a LM19.1 blade at wind speeds of (a) 7, (b) 10 and (c) 12 m/s.

To check the flow behaviours in the region near the tip, limiting streamlines in a zoomed region are plotted in Figure 2. The figure shows that the flow near the tip at a wind speed of 7 m/s is almost attached. When the wind speed increases to 12 m/s, the tip flow is separated.

The normal and tangential forces are plotted in Figure 3. The normal and tangential forces increase with wind speed and the tangential force is much smaller than the normal force.

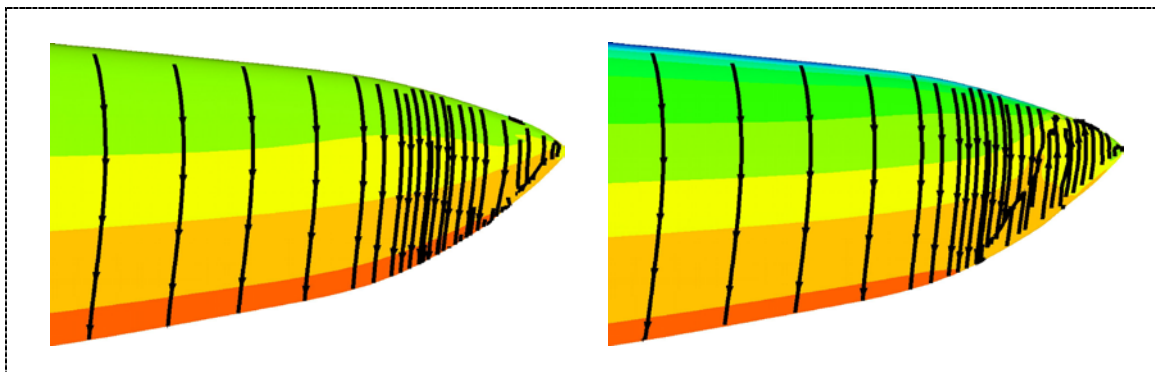
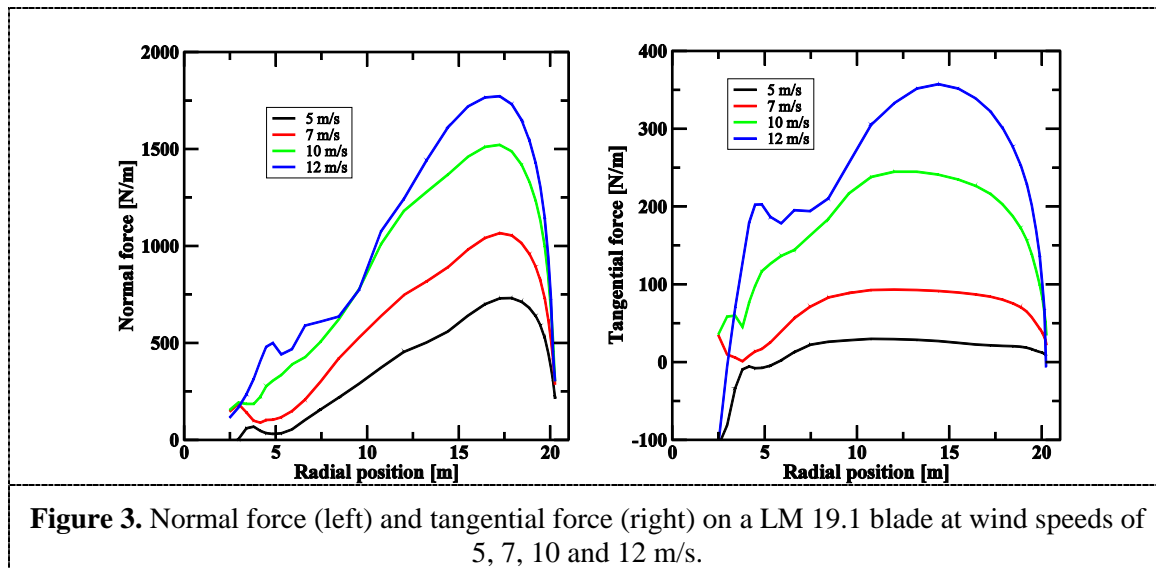
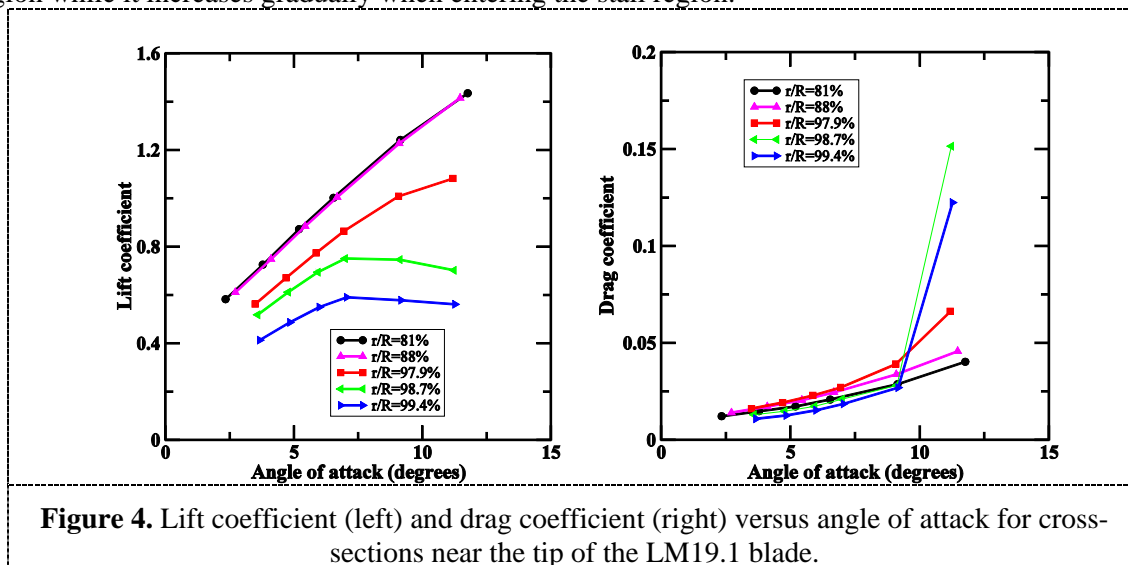


**Figure 2.** Limiting streamlines in the tip region of a LM19.1 blade at wind speeds of 7 (left) and 12 (right) m/s.



By using the technique of determination of the angle of attack [5], the angle of attack can be derived. In Figure 4, the extracted lift and drag force coefficients are shown in function of the angle of attack. The figure shows that the lift decreases gradually when close to the tip and the flows at wind speeds of 10 and 12 m/s are stalled at the tip. For the drag coefficient, it does not change significantly in the tip region while it increases gradually when entering the stall region.



### 5.2. New Tip loss function

In order to follow the changes in lift coefficient for blades with sharp tip while keeping the same properties for blades with blunt tip, the tip loss function is modified to

$$F_1 = \frac{2}{\pi} \cos^{-1} \left[ \exp\left(-g \frac{B(R-r)^n}{2r^n \sin \phi}\right) \right] \quad (5)$$

$$g = \exp\left(-\frac{0.125(B\lambda - 21)}{1 - 2 \min(dc/dr)}\right) + 0.1 \quad (6)$$

where  $dc/dr$  is the gradient of the chord distribution in the radial direction in the tip region and the exponent  $n$  is

$$n = 1 + 0.5 \min(dc/dr) \tag{7}$$

It is worth noting that for a blade with a blunt tip ( $dc/dr \approx 0$ ), equations (5)-(7) reduce to equations (3)-(4). As the blade shape at tip is not well defined, we assume  $dc/dr \approx -0.45$  in our study.

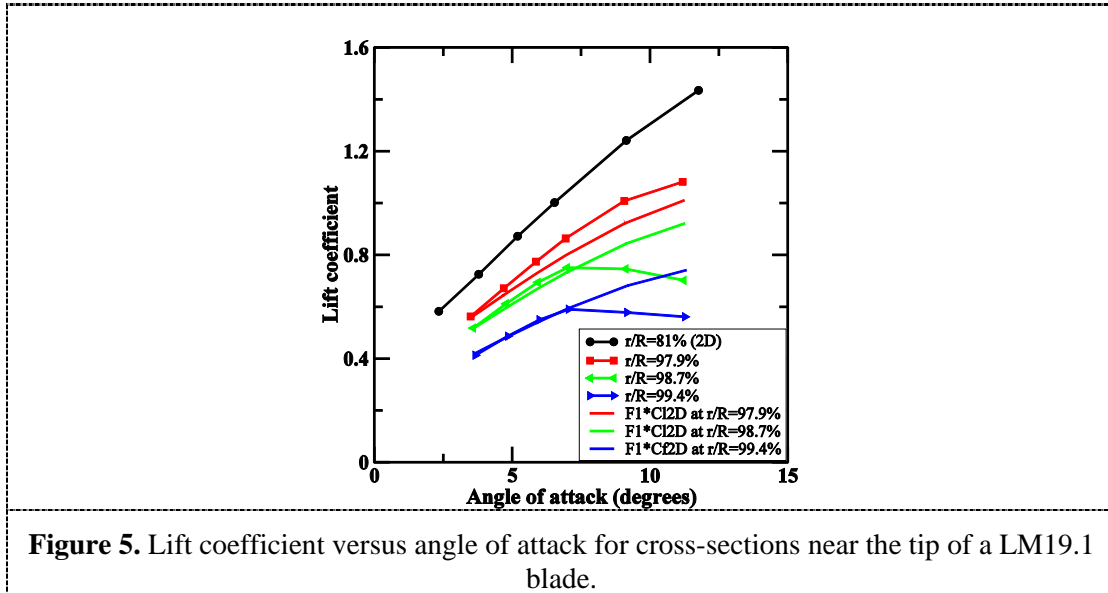


**Figure 5.** Lift coefficient versus angle of attack for cross-sections near the tip of a LM19.1 blade.

Applying the new tip loss function (Equations (5)-(7)) and using the lift force coefficients at  $r=88\%R$  as the corresponding 2D airfoil characteristics, the obtained lift coefficient is plotted in Figure 5. It is seen that the lift force obtained with the new F1 fits well with the derived lift force coefficient on the blade at  $r/R=97.9\%$ . At  $r/R=98.8\%$  and  $99.4\%$ , they fit quite well at small angles of attack and the deviation increases when stall appears.

### 5.3. Validation of BEM against CFD

To check if the newly derived tip loss function can be used for the performance prediction of wind turbines with sharp blade tip, BEM computations for the NordTank 500 kW turbine and for the NREL 5MW turbine are carried out in this section. The former case is considered to be a validation check while the latter case is considered as an application.

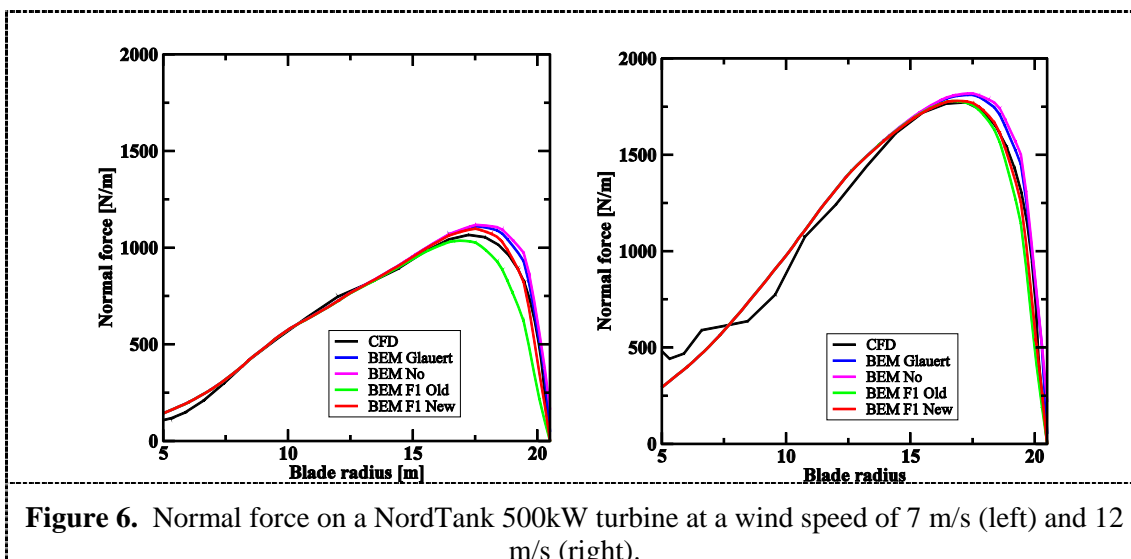
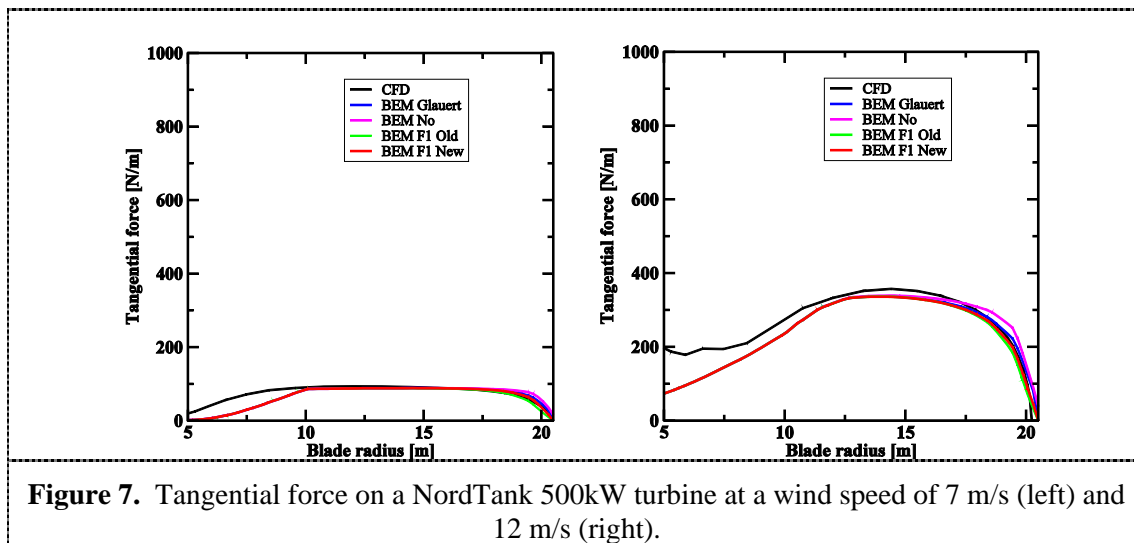


**Figure 6.** Normal force on a NordTank 500kW turbine at a wind speed of 7 m/s (left) and 12 m/s (right).



### 5.3.1. BEM computations for flows past the NordTank 500kW turbine

BEM computations for flows past the Nordtank 500 kW turbine are carried out. The obtained normal force at wind speeds of 7 m/s and 12 m/s is compared to that from the CFD computations and shown in Figure 6. For comparison reasons, BEM computations with Glauert tip loss correction (BEM Glauert), without tip loss correction (BEM No) and with the old F1 function (BEM F1 Old) are also plotted in the figure. BEM with the new F1 function (BEM F1 New) is seen to predict correctly the force near the blade tip while BEM F1 Old under-predicts the loading. BEM Glauert and BEM No over-predict the normal force at the tip. The tangential force is plotted in Figure 7. From the figure, it is seen that all models give similar results except that BEM No over-predicts the tangential force.

### 5.3.2. BEM computations for flows past the NREL 5MW turbine

As a prediction, BEM computations with the new F1 function for flows past the NREL 5 MW turbine [16] are carried out. To make a comparison, CFD computations for this turbine are also carried out. The mesh used for the NREL 5MW rotor is a cylindrical mesh which covers a domain with radius of 245 m and inlet and outlet located at 287 m in front and behind the rotor, respectively. To reduce the computing cost, only one blade is meshed and periodic boundary conditions are used to take into account the influence from the other two blades. To resolve the boundary layer, the first cell height from the blade surface is kept to below  $10^{-5}$  m. The total number of mesh points for the virtual NREL 5MW rotor is about  $4.2 \times 10^6$ .

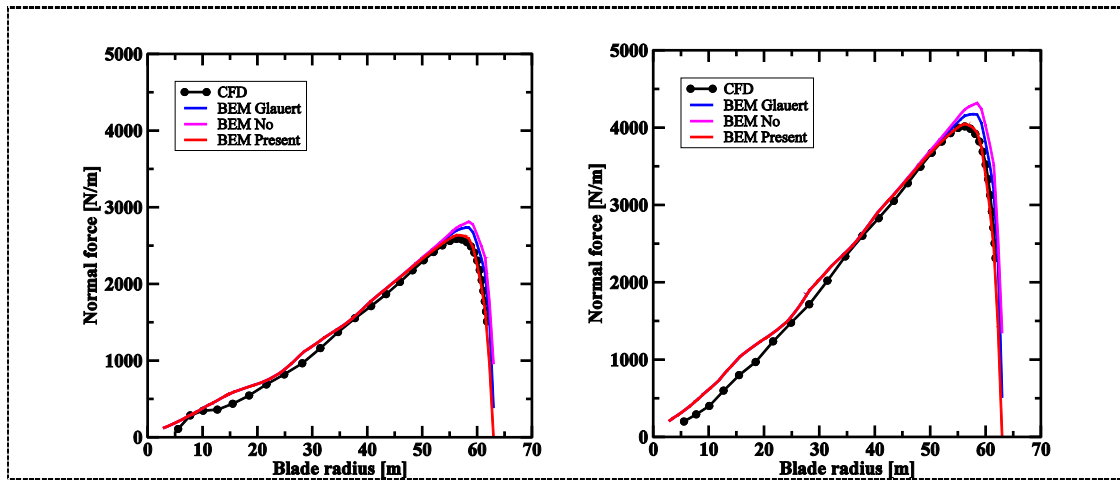


Figure 8. Normal force on the NREL 5MW turbine at a wind speed of 6 m/s (left) and 8 m/s (right)

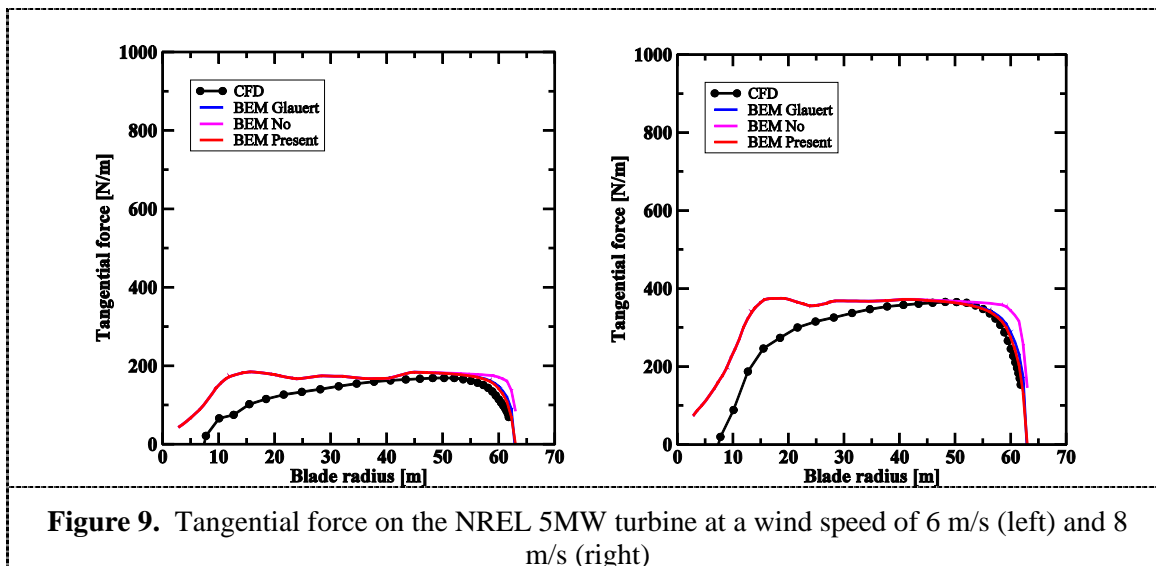


Figure 9. Tangential force on the NREL 5MW turbine at a wind speed of 6 m/s (left) and 8 m/s (right)

The obtained normal force at wind speeds of 6 m/s and 8 m/s is compared to that from CFD computations and shown in Figure 8. For comparison, “BEM Glauert” and “BEM No” are also plotted in the figure. “BEM F1 New” is seen to predict correctly the force near the blade tip. “BEM Glauert” and “BEM No” over-predict at the tip. The tangential force is plotted in Figure 9. From the figure, it is seen that all models give similar results except that “BEM No” over-predicts the tangential force.

## 6. Conclusions

In this paper, tip loss effects on wind turbine blades with sharp tip have been studied using CFD computations. As CFD provides detailed information in the blade tip region, the derived airfoil data are successfully used for deriving a new tip loss correction function. The derived tip loss function F1 is then implemented in a standard BEM code. BEM computations have been carried out for a NordTank 500 kW turbine and the NREL 5MW turbine and excellent agreements with CFD results are seen. To further validate the F1 function, more comparisons with CFD results will be made later.

## 7. References

- [1] Shen W Z, Mikkelsen R, Sørensen J N and Bak C 2005 Tip loss corrections for wind turbine computations *Wind Energy* **8** 457-475
- [2] Shen W Z, Mikkelsen R and Sørensen J N 2005 Tip loss correction for Actuator / Navier-Stokes computations *Journal of Solar Energy Engineering* **127** 209-213
- [3] Giguere P, Selig M S 1999 Design of a tapered and twisted blade for the NREL combined experiment rotor *NREL Report SR-500-26173* National Renewable Energy Laboratory Colorado
- [4] Ronsten G, Dahlberg J, Meijer S, He D X, and Chen M 1989 Pressure measurements on a 5.35 m HAWT in CARDC 12 · 16 m wind tunnel compared to theoretical pressure distributions *Proceeding of European Wind Energy Conference and Exhibition (EWEC 89)* Glasgow 729-735
- [5] Shen W Z, Hansen M O L and Sørensen J N 2009 Determination of the angle of attack on rotor blades *Wind Energy* **12** 91-98
- [6] Michelsen J A 1992 Basis3D – A platform for development of multiblock PDE solvers. *Technical Report AFM 1992-05* Technical University of Denmark
- [7] Sørensen N N 1995 General purpose flow solver applied over hills *RISØ-R-827(EN)* RISØ National Laboratory Roskilde Denmark
- [8] Shen W Z, Michelsen J A, and Sørensen J N 2001 An improved Rhie-Chow interpolation for unsteady flow computations *AIAA Journal* **39** 2406-2409
- [9] Menter F R 1994 Two-equation eddy-viscosity turbulence models for engineering applications *AIAA Journal* **32** 1598-1605
- [10] Prandtl L 1927 *Vier Abhandlungen zur Hydrodynamik und Aerodynamik* Göttinger Nachr Göttingen 88-92
- [11] Glauert H 1963 Airplane propellers In *Aerodynamic theory* Durant WF (ed) Dover New York 169-360
- [12] Hansen M O L 2000 *Aerodynamics of wind turbines* Published by James & James (Science Publishers) Ltd UK
- [13] Wilson R E and Lissaman P B S 1974 *Applied aerodynamics of wind power machines* Oregon State University Report NSF/RAN-74113
- [14] De Vries O 1979 *Fluid dynamic aspects of wind energy conversion* AGARD Report AG-243
- [15] Johansen J and Sørensen N N 2004 Airfoil characteristics from 3D CFD rotor computations *Wind Energy* **7** 283-294
- [16] Jonkman J, Butterfield S, Musial W and Scott G 2009 Definition of a 5-MW reference wind turbine for offshore system development *Technical Report NREL/TP-500-38060*

## Acknowledgments

This work was supported by the Energy Technology Development and Demonstration Program (EUDP-2011-I, J. nr. 64011-0094) under the Danish Energy Agency.